

## Supporting Information

### Flexible Anti-Clogging Graphite Film for Scalable Solar Desalination by Heat Localization

Varun Kashyap, Abdullah Al-Bayati, Seyed Mohammad Sajadi, Peyman Irajizad, Sing Hi Wang and Hadi Ghasemi

*Department of Mechanical Engineering, University of Houston, 4726 Calhoun Rd, Houston, Texas, 77204, USA.*

*E-mail: hghasemi@uh.edu*

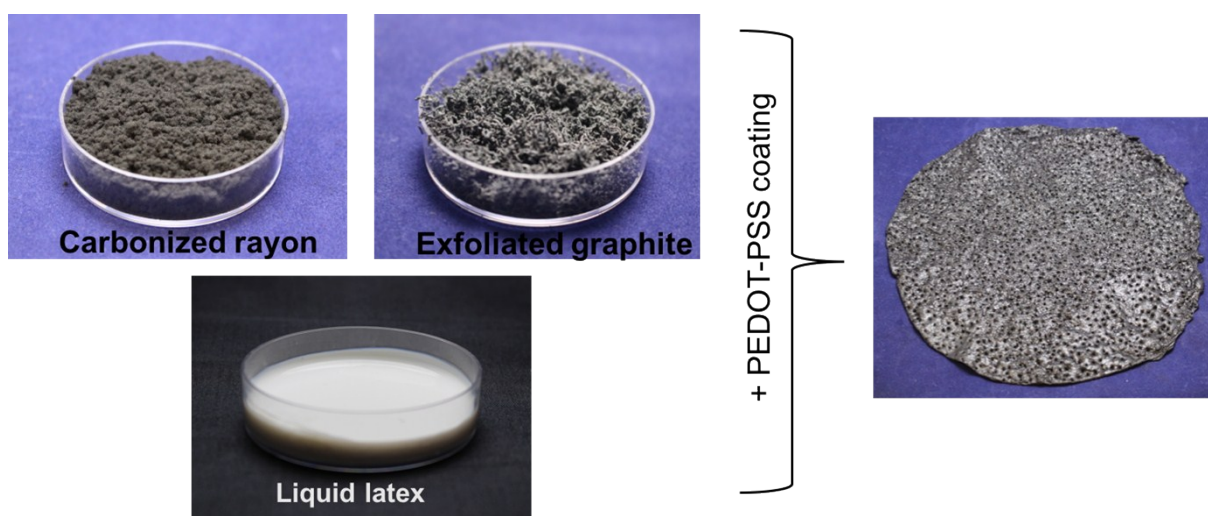


**Figure S1:** The components for development of ACSD are shown. Latex provides a low thermal conductivity skeleton. The graphite flakes and the carbon fibers lead to heat localization at the liquid-vapor interface and integrity of the structure. Note that without carbon fibers, the exfoliated graphite cannot form a homogenous structure with latex polymer.

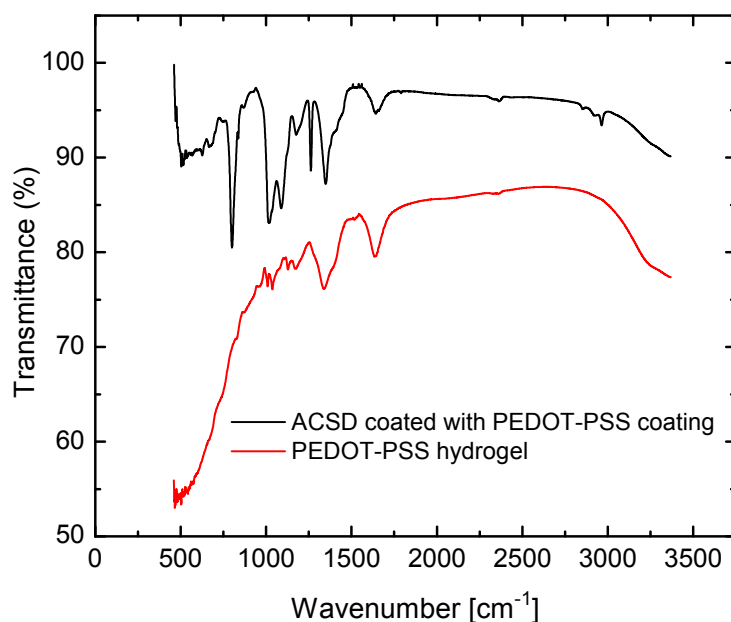


**Figure S2:** FTIR spectrum of ACSD is examined. The spectrum includes the peaks by PEDOT-PSS along with peaks from carbon structure and liquid latex matrix.

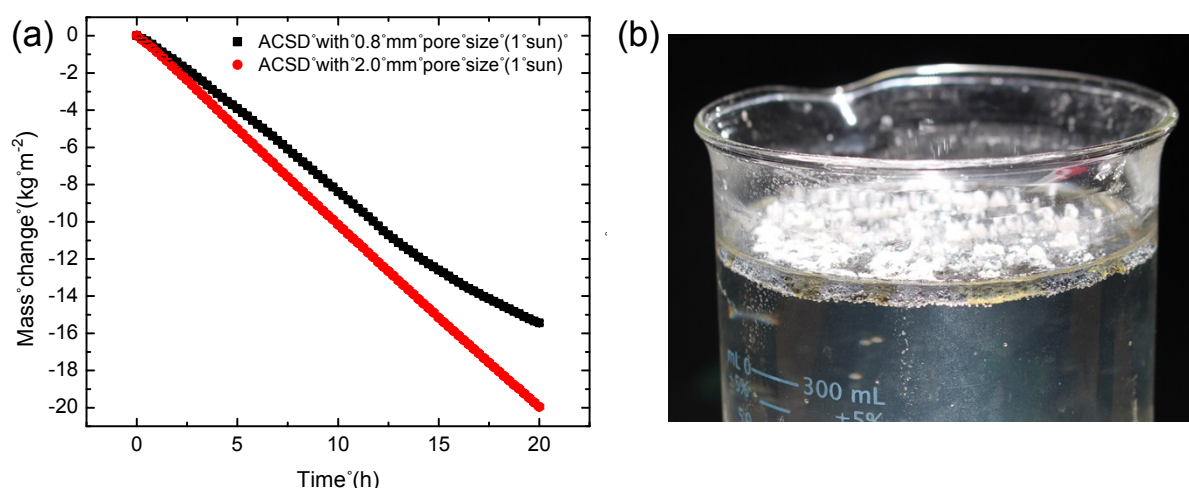


**Figure S3:** (a) Role of pore dimension on performance of ACSD is shown. With small pores, there is no passage for the free fall of precipitated salt particles, thereby reducing the evaporation rate. Note that both structure are coated with PEDOT-PSS. (b) Salt accumulation on the material structure is shown. For small pore dimensions, the salt particles accumulate at the surface and deter the performance of the structure. The vapour flux for ACSD with 0.8 mm pore size in short duration ( $<15$  hr) and long duration ( $>15$  hr) are  $0.83$  and  $0.48 \text{ kgm}^{-2}\text{h}^{-1}$ , respectively. This flux for ACSD with 2.0 mm pore dimension is  $1.01 \text{ kgm}^{-2}\text{h}^{-1}$ .

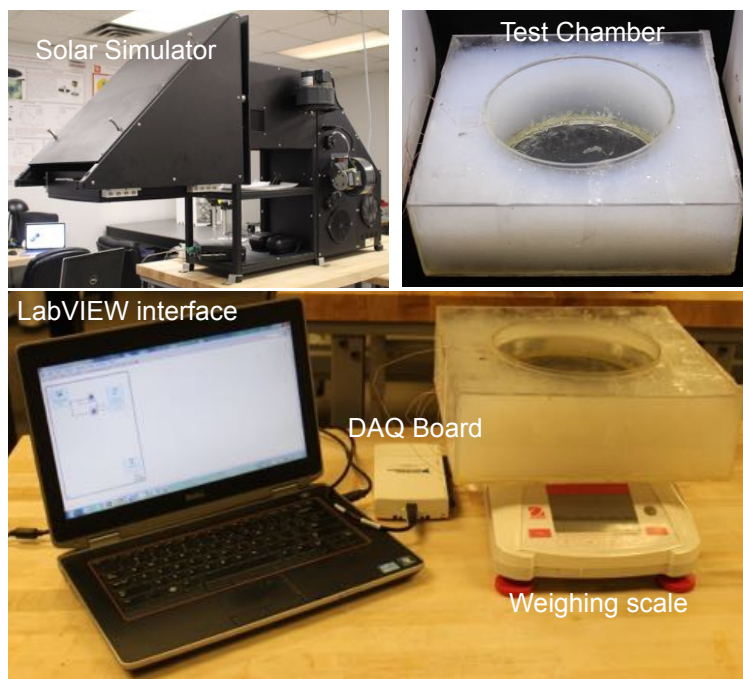


**Figure S4:** The experimental setup to conduct evaporation experiments is shown. The experimental setup is custom-designed to minimize the side losses. The evaporation rate and temperature field in the vapor and the liquid are measured through a Labview program.

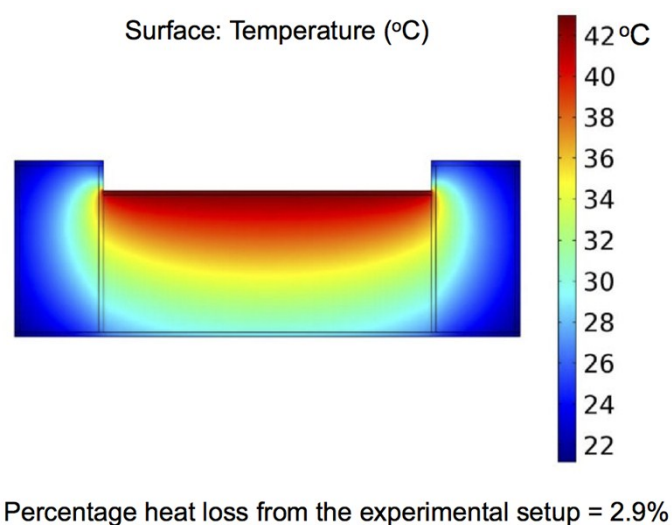


**Figure S5:** Temperature field in the experimental setup is simulated. As the sides are insulated with aerogel particles, the major loss is through the liquid medium and accounts for 2% while ACSF surface temperature is 43 °C.

### **Thermal conductivity measurements**

Thermal conductivity is measured using the IR method reported earlier. ACSD is placed between two glass slides of known thermal conductivity for reference. A resistance heater is placed on top of the sample and the current is varied to set a range of temperature gradients across the sample. A pre-calibrated IR camera (FLIR SC7000) with a resolution of 25  $\mu\text{m}$  is placed in front of the sample to measure the temperature gradient in the glass slab and ACSD. Knowing the thermal conductivity of the reference material ( $1.4 \text{ Wm}^{-1}\text{K}^{-1}$ ) and the temperature gradient in the glass slide, the heat flux to ACSD is calculated. Given the heat flux, and temperature gradient across the material, the thermal conductivity of ACSD was calculated using the Fourier equation.

### **Experimental setup for evaporation rate experiment**

The experimental setup required to evaluate the evaporation rate of ACSD on a lab scale is shown in **Figure S4**. The experimental setup is equipped with a solar simulator which includes an optical head (OAI 0131-0293-01 with Aluminum mirror and 1.6 kW lamp), a power measurement system consisting of a Newport thermopile detector (919P-500-65, 500W, 65 mm diameter) and Newport power meter (1918-R), thermocouples k-type for measurement of liquid and vapor temperatures, a data acquisition system (National Instruments, NI USB-6210), a test container, and a balance (OHAUS Adventurer AX8201).

The designed test setup is shown in **Figure S4**. Acrylic tubing with 8” (20.32 cm) diameter was used in the test setup for its low thermal conductivity. The external box was fabricated using acrylic sheets with 12” (30.48 cm) length on each side. The gap between the box and the tube was filled with translucent hydrophobic aerogel particles (Cabot Lumira LA-1000). Aerogel was used to provide thermal insulation and minimize side losses. The balance with 0.1 g accuracy was used to measure the mass loss due to evaporation and determine the thermal efficiency. Type K thermocouples were used for the measurement of liquid and vapor

temperatures. Four of these thermocouples were placed in the acrylic tube with 2 cm distance between them to measure the conduction loss to the underlying liquid. The fifth thermocouple was placed on top of ESE to measure the vapor temperature. These were connected to a data acquisition system (*National instruments, NI USB-6210*) and the generated data was collected using a LabView program. The solar irradiation is measured using the thermopile and the power meter. The error in the solar illumination at the illuminated spot is measured using a OAI 340 solar meter and  $< 3\%$  error was observed.

### **Heat transfer simulation**

The heat loss of the experimental setup intended to evaluate the performance of ACSD on the lab scale is modeled on COMSOL. The boundary conditions included a convective boundary condition with  $h = 10 \text{ Wm}^{-2}\text{K}^{-1}$  at the walls, top and bottom surface of the test chamber excluding the evaporating surface, a boundary heat flux of  $1000 \text{ Wm}^{-2}$  (1 sun) at the top surface of ACSD where the solar irradiation is simulated. The ACSD is about 1.2mm thick and have thermal conductivity of  $0.56 \text{ Wm}^{-1}\text{K}^{-1}$  as measured above. The thermal conductivities of the walls (acrylic) and aerogel insulation are considered to be  $0.2 \text{ Wm}^{-1}\text{K}^{-1}$  and  $0.02 \text{ Wm}^{-1}\text{K}^{-1}$  respectively. The temperature distribution obtained from this simulation is shown in **Figure S5**. Through these simulations, we found that the heat loss to the experimental setup is 2.9 %.